SEMARAK ILMU PUBLISHING

Journal of Advanced Research in Applied Mechanics

Journal homepage:
https://semarakilmu.com.my/journals/index.php/appl_mech/index
ISSN: 2289-7895

Ultra-Narrow Gap Welding Process Experiment of Underwater Cast Steel Pipeline

Xiaotong Han[1], Liang Zhu[2], Xiaoxia Jiang[3], Wei Han Khor[1], Hooi Siang Kang[1,*]

[1] Faculty of Mechanical Engineering Universiti Teknologi Malaysia, 81310 Johor Bahru, Malaysia
[2] School of Materials Science and Engineering, Lanzhou University of Technology, Lanzhou 730050, China
[3] School of Mechanical Engineering Ningxia University, 750021 Yinchuan, China

ARTICLE INFO

Article history:
Received 23 April 2024
Received in revised form 18 June 2024
Accepted 1 July 2024
Available online 30 July 2024

Keywords:
Ultra-narrow gap welding; flux band; welding parameters; microstructure; welded joint

ABSTRACT

The installation and laying of underwater pipelines are the cornerstone of ocean engineering. They are crucial to the distribution of important fossil energy sources such as oil and natural gas around the world. Welding technology is an indispensable part of pipe connection. A new welding method is proposed to improve the quality of welded joints of underwater cast steel pipelines, which is the flux band-constrained arc ultra-narrow gap welding (UNGW) method. UNGW has unique welding advantages compared to traditional welding methods, including high welding efficiency, excellent welding joint performance, small welding deformation, and low welding heat input. The experimental study on UNGW for the application of underwater cast steel pipeline is conducted by manipulating the welding parameters, such as the welding arc voltage and welding current, and observing the microstructural and mechanical properties of the weld. The optimal range of welding parameters for weld formation are welding voltage of 22 V, welding current of 200-230 A, and welding speed of 8.25-9 mm/s. The microstructure analysis of the welded joints observed a mixture of tempered martensite, bainite, and retained austenite are detected at Heat Affected Zones (HAZ), whereas the results of microhardness showed no softening occurred in the welded joints. The composition of the flux band can be manipulated to improve the fusion of air bubbles and side walls.

1. Introduction

In recent years, there has been a significant increase in underwater oil and gas development, and renewable energy with exploration and production activities experiencing a notable surge, driving advancements in technology and investment [1-4]. Pipeline transport is widely regarded as the most common, economical, and safe method for moving oil and natural gas. As of 2022, the global network of pipelines extended over 2.06 million kilometers. The United States, Russia, and China lead in pipeline infrastructure, collectively boasting about 180,000 kilometers. This extensive development highlights pipelines' critical role in global energy supply chains, offering a reliable and cost-effective

* *Corresponding author.*
E-mail address: kanghs@utm.my

https://doi.org/10.37934/aram.122.1.113

solution for fuel transportation, minimizing environmental risks and ensuring steady delivery across vast geographical areas [5]. Pipe-laying barges serve as mobile platforms for laying pipelines underwater. It is equipped with alignment, welding, and other mechanisms internally. After completing the welding work at the welding station inside the barge, it is laid in the designated underwater area with S-lay or J-lay [6].

Commonly used welding methods for the internal welding of pipeline barges include shielded metal arc welding (SMAW), gas tungsten arc welding (GTAW), and flux-cored arc welding (FCAW) [7-8]. Each welding method has its own pros and cons. SMAW is favored for its simplicity and versatility. Despite this, electrodes need to be replaced frequently throughout the welding process, resulting in decreased production efficiency and increased labor costs. Such frequent interruptions can significantly extend the duration of a construction project and increase overall expenses [9]. GTAW requires a preset V-groove during welding. As the thickness of the pipe wall increases, the angle and depth of the V-groove will increase, which complicates the overall welding process. The likelihood of encountering welding defects increases when performing single-pass multi-layer welding [10]. FCAW produces a large amount of smoke during the welding process, and after the welding is completed, the smoke will remain inside the weld metal to form air bubbles [11]. These air bubbles will lead to a decrease in the quality of the welding.

The conventional welding methods described above will cause different types of welding defects in the welding metal. Jiang *et al.,* [12] explained that welding defects are divided into plane defects and volume defects. Flat defects include cracks, lack of fusion, and undercuts with a depth greater than or equal to 1 mm. Volume defects include pits with a depth of <1mm, bubbles, slag inclusions, and so on. Pipes with welding defects are at increased risk of fracture when exposed to the harsh underwater environment [13]. These defects not only affect the structural integrity of the welded components but also pose serious safety concerns, which require careful inspection and quality assurance measures throughout the welding process. For instance, cracks inside and outside the weld serve as fracture initiation points [14]. Cyclic stresses generated by associated thermal changes in water flow, pressure fluctuations, depth, and water temperature cause weld cracks to expand over time, ultimately leading to pipe fracture [15]. The presence of air bubbles creates small voids inside the weld. Water trapped in air bubbles can cause electrochemical corrosion [16]. This results in a decrease in the mechanical properties of the welded joint and a shortened service life. Slag inclusions and incomplete fusion lead to weak welded joints. Failures can occur under the classic mechanical loads and dynamic pressures found in underwater environments leading to direct rupture of the pipe [17].

Flux-bands constrained arc ultra-narrow gap welding (UNGW) technology is a major advancement for the application in underwater pipeline installation, improving productivity and structural integrity. Conventional welding methods, while effective, often have limitations that hinder efficiency and affect quality [18]. UNGW has the potential in meeting these challenges whilst achieving good results. UNGW requires a preset I-groove which does not change as the pipe wall thickness increases. By reducing the gap size between the pieces to be welded, the amount of filler material required is minimized, which not only reduces costs but also speeds up the welding process [19]. The efficiency of this filler material use results in shorter overall welding times and less thermal distortion, thus maintaining the mechanical and structural properties of the base material [20]. Additionally, UNGW reduces the heat input required for welding. Lower heat input minimizes the width of the heat-affected zone (HAZ), maintaining the integrity of the surrounding metal and reducing the risk of thermal distortion and residual stress [21]. This aspect is critical to maintaining the dimensional stability and mechanical strength of critical structures. UNGW typically has a narrower gap than traditional welding techniques and uses flux bands to constrain the arc generated

during welding and prevent it from rising, thus minimizing the chance of welding defects. A narrower molten pool is easier to control and monitor during the welding process, resulting in improved welding quality [22].

For instance, Li *et al.,* [23] studied molten pool formation in ultra-narrow gap welding. The research results show that as the welding current increases, the transition form changes from short-circuit transition to a mixture of short-circuit transition and spherical transition and then to spray transition. The relationship between the droplet transfer process and welding defects to obtain high-quality welds with a stable transfer process. On the other hand, Gong *et al.,* [24] studied flux band restraint and arc action mechanisms. Research shows that when the melting area of the flux band is greater than a certain value but smaller than the shrinkage area of the wall, a suitable degree of arc shrinkage can be obtained, and the arc heating area can be controlled at the bottom of the groove and the side wall to form a well-formed weld. When the melting area is larger than the wall shrinkage area, the degree of arc shrinkage decreases, and the arc heating area is limited to both sides of the wall, making it difficult to form a complete molten pool. The result is a weld with lots of holes.

The arc properties and transitions of UNGW droplets are researched by Chen *et al.,* [25]. Arc length affects heat input and arc stability; an arc that is too short or too long can lead to arc instability, spatter, or insufficient penetration. Flux bands constrained arc ultra-narrow gap welding technology has been successfully used in the welding of U17Mn train rails[26]. Through the analysis of a large amount of welding experimental data, the corresponding process specifications were obtained [27].

Previous studies showed that there is a need to address the relationship between welding parameters and the weld forming quality when studying UNGW. Therefore, leading to the importance of this study to determine the optimal range of welding parameters, while expressing the weld quality in terms of microstructure, mechanical properties and formation of bubbles. This study aims to determine the important parameters of flux band-constrained arc UNGW for the application of underwater cast steel pipelines and analyze whether the welding forming effect can meet the challenges of complex underwater environments. The results are expected to provide theoretical support for implementing UNGW in underwater cast steel pipe. In particular, the UNGW welding parameters of the underwater cast steel pipeline, the microstructure of the weld metal, the mechanical properties of the weld metal, and the formation of bubbles inside the weld are to be studied, to improve the welding process and avoid the generation of air bubbles inside the weld.

2. Methodology

2.1 Materials and Specimen Preparation

The base material used in this study is ZG13Cr9MoV cast steel pipe. The chemical composition of this material is shown in Table 1. The welding wire used was Φ1.6 mm H08Mn2Si heat-resistant steel wire. A material preparation process was conducted during the pre-welding process. The sample for this experiment is pre-set with an I-joint with a gap width of 5mm, while 0.7mm flux bands are pre-placed on the left and right walls of the joint root. A welding wire with a diameter of Φ1.6mm is used as the melting pole and electrode for arc welding. For the pre-welding process, the oxides are first removed from the welded side and the surface of the parent material. Then the welded side and the surface of the parent material were wiped with alcohol and acetone to remove oil and dirt. Finally, the material was kept dry and at a constant temperature suitable for welding.

After the welding process, a specimen of 20mm×20mm×60mm at the welding of the cast steel was collected for the analysis of microstructure. The specimen was grinded and polished, then it was corroded with 4% nitric acid (HNO_3) in alcohol solution and kept for the phenomenon of fogging on the metal surface to stop corrosion. Later, the specimen was cleaned up using distilled water to

remove residual corrosion solution on the metal surface. Alcohol was applied to wipe the metal surface of the specimen, and then the specimen was dried out using a dryer. The specimens are used for microstructure analysis.

Table 1
Chemical composition (%) for ZG13Cr9MoV parent materials and H08Mn2Si welding wire

	ZG13Cr9MoV based material	H08Mn2Si welding wire
C	0.13	0.13
Si	0.08	0.30
Mn	0.4	0.75
S	0.002	0.01
P	0.005	0.02
Cr	9.26	9.11
Mo	1.5	1.59
Co	1.13	1.15
Ni	0.14	0.02
V	0.20	0.21
Nb	0.05	0.05
N	0.02	0.01
B	0.009	0.01

2.2 Welding Process

A schematic diagram of UNGW is shown in Figure 1. The flux tape was pre-positioned on both sides of the angle with a gap width of 5 mm. The flux bands were made of flux band and glass fiber mesh bonded together and were bent into a U-shape by using the reaction force of the glass fiber mesh to keep the flux sheets tightly attached to both sides of the bevel. Welding strip structure and prefabrication methods are keys to the stability of UNGW [28]. The process of making the flux band used in this experiment includes powder screening, powder mixing, drying, press molding, and drying [29]. The flux band is similar in composition to the alkaline flux band used in manual arc welding whose main components are marble and fluorite [30]. The chemical composition of the flux bands as shown in Table 2.

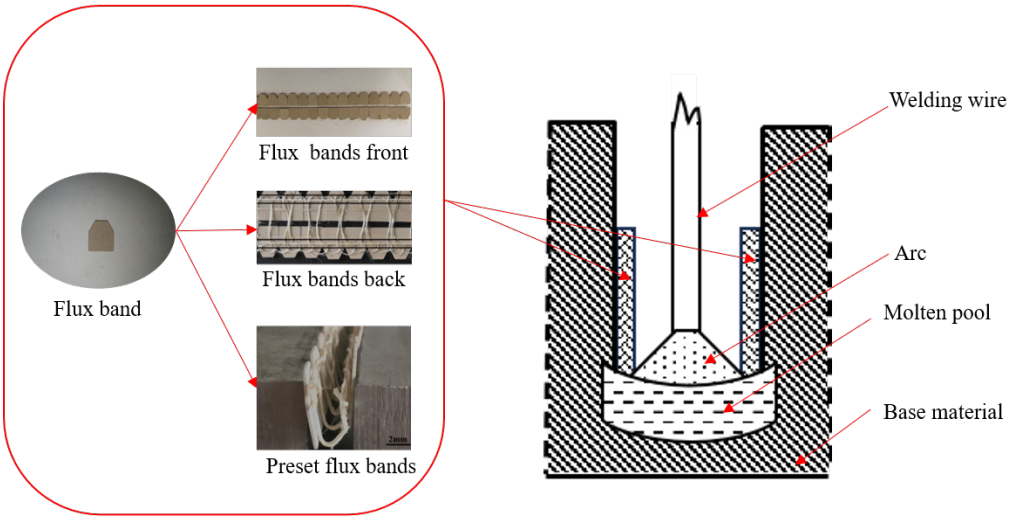

Fig. 1. Schematic diagram of ultra-narrow gap welding

Table 2
Chemical composition (%) of the flux band

Marble	45
Fluorite	31
Titanium dioxide	10
Potassium silicate	5
Others	9

The welding device was set up on the workpiece to be welded, then the welding power supply was switched on to start welding. During the welding process, the high temperature generated by the arc will melt about 40-60% of the flux bands, the resulting slag and stable gas to the weld metal play a protective role in preventing welding oxidation, and the flux band in the process of melting can take away a certain amount of heat and thus make the arc contraction. For non-melted flux band, the arc plays a role as a mechanical constraint, whereas, the bevel side walls of the weld base material and wire insulation prevent the arc from climbing [31].

Partial melting of the flux bands starts at 650 °C and the temperature rises to 800 °C when it transforms from a solid to a gas-liquid mixture. The flux bands decompose at high temperatures to produce CO_2 gas and slag containing calcium (Ca) compounds [32], which has the effect of self-generating slag and gas and protects the welding process. The flux bands also have a thermal compression effect on the arc as the melting of the flux band takes away some of the heat from the arc.

3. Results and Discussion

The welded specimens were prepared and observed on the fusion between the bevel and the sidewall. Figure 2 shows a schematic diagram of the weld fusion pattern, the maximum fusion width *b*, the fusion depth of the base material *d*. The fusion depth of the sidewall *s* was measured.

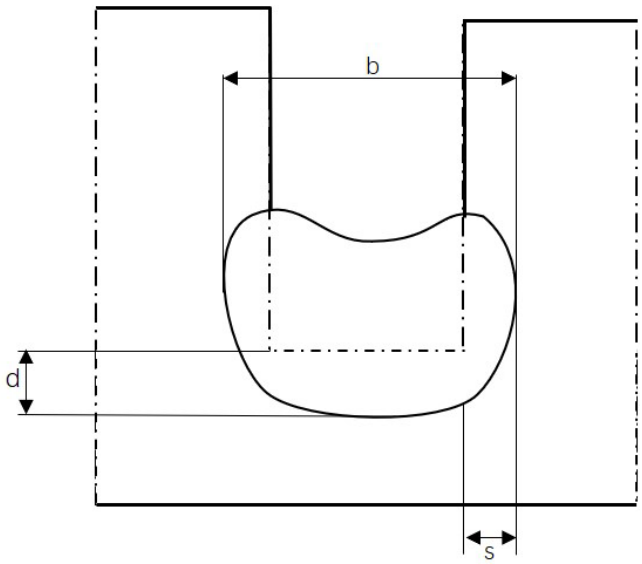

Fig. 2. Weld fusion pattern

3.1 Effect of Welding Parameters on Weld Morphology

Individual variations of welding parameters have a different effect on the fusion of the weld metal with the walls on both sides. The experimental results obtained with different arc voltages were

analyzed with no change in other parameters. The welding current used in this experiment was 200 A, the bevel width was 5 mm, the welding speed was 8.6 mm/s, and the welding arc voltages were 21.5 V, 22.0 V, and 23.5 V, respectively. As the arc voltage increases, the depth of melting at the root of the bevel, *s* increases, the depth of melting of the base material, *d* decreases, and the maximum degree of melting, *b* increases. On the other hand, when analyzing the experimental results obtained from different welding currents while keeping other parameters constant, the angle melting depth *s*, the base metal melting depth *d*, and the maximum melting depth *b* tend to increase as the welding current increases. For the experiment of varying welding currents, the arc voltage used in this experiment is 22 V, the bevel width is 5 mm, the welding speed is 8.6 mm/s and the welding currents are 200 A, 215 A, and 225 A, respectively.

Figure 3 shows the relationship between arc voltage, welding current, and weld seam morphology. When the arc voltage is less than 21.5 V, under the condition that the diameter of the welding arc is smaller than the gap width of the bevel, therefore the poor fusion of the sidewalls, and the welding seam is in a concave state. On the other hand, while the arc voltage is greater than 23 V, the arc was elongated and the flux band was burned completely, which led to the flux band cannot constrain to the arc so that the arc was in a climbing phenomenon, and therefore this cannot form a complete weld. The climbing phenomenon can cause a risk of damage to the torch as well. Therefore, the arc voltage range that is applicable for steel pipes is between 21.5 V and 23 V.

For the welding current less than 200 A, the angle on both sides of the heat input is reduced, resulting in poor fusion of the slope. On the other hand, for welding current greater than 230 A, the weld pool area is large, and therefore the molten pool, under the effects of the external force, will produce a flow and resulting a poor fusion. These poor fusions will make air bubbles trapped during the welding process. From Figure 3, when the arc voltage was found to be between 21.5 V–23 V to get a stable welding arc. However, when the related welding current was less than 200 A, the welding fusion is incomplete and prone to welding defects such as biting edge. When the related welding current is greater than 230 A, the large-size liquid weld is easily affected by the external force and causes the weld metal to be in convex form, which leads to a poor fusion after the weld cooling down. Therefore, the range of the welding current that is applicable for steel pipes is between 200 A and 230 A. A good fusion was obtained when the setting of voltage and current were 22 V and 215 A, respectively, and the welding speed of 8.6 mm/s, weld width of 5 mm. The cross-section area for the weld fusion for a single-pass multi-layer welding is shown in Figure 4.

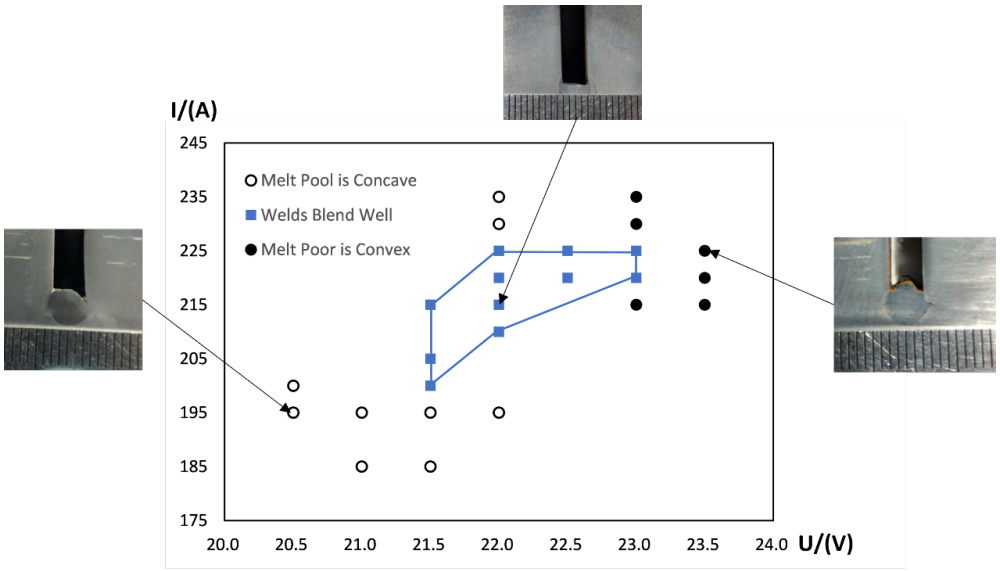

Fig. 3. Current and voltage relationship diagram

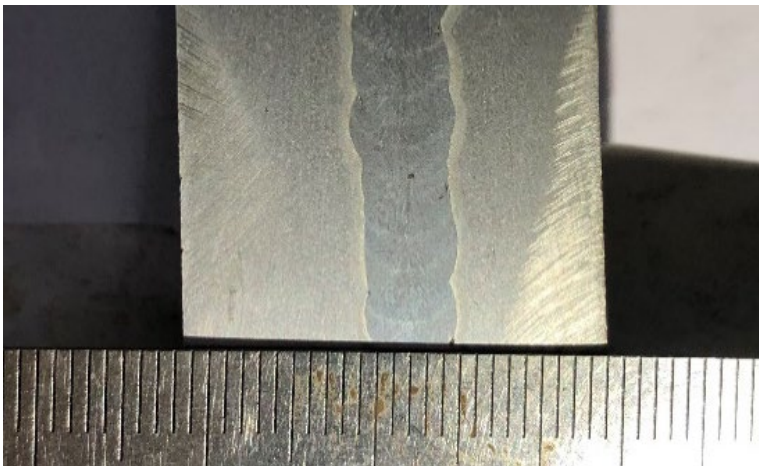

Fig. 4. Cross-sectional area of a good fusion for single-pass multi-layer welding

3.2 Microstructure of Welded Joints

Microstructure analysis in welded joints involves the examination of structure in the microscopic arrangement, such as the arrangement of grains, phases, and defects within the weld and its surrounding areas, especially at the heat-affected zone (HAZ). During welding, the base material undergoes significant thermal cycles, which can lead to various microstructural transformations, such as grain growth, phase changes, and the formation of new constituents. The formation of distinct grain structures influences the mechanical properties of the joint, whereas phase formations are critical in determining the weld properties. Early detection of weld defects during the microstructure analysis is also essential in the study of the integrity of the weld. Most importantly, the microstructure at the HAZ should be investigated as it highly affects the mechanical properties of the weld.

The microstructural characteristics of different regions of ZG13Cr9MoV cast steel welded joints were studied. As shown in Figure 5a, the microstructure shows clear changes in morphology and grain size between the weld zone, heat-affected zone, and the base material. The microstructural pattern of the weld zone is greatly influenced by the high temperatures generated during the welding process. This high heat input causes the grains in the weld zone to recrystallize, generally resulting in larger, more uniform grains compared to the surrounding areas. In the HAZ, the microstructural properties are affected by the thermal gradient between the weld zone and the parent metal. Here, the metal experiences temperatures high enough to change its microstructure, but not to the melting point. This results in partial recrystallization, often producing grains of different sizes and morphology. The HAZ typically contains grains that are finer than the weld zone but coarser than the parent metal.

Inferred from the mechanical properties exhibited and microscopic observations. The microstructure of the based material is martensite and ferrite in the normalized state as shown in Figure 5b. Their presence is a testament to the wear resistance, corrosion resistance, ductility, and toughness of the base material. The microstructure of the weld is acicular martensite and lamellar as shown in Figure 5c. During the weld forming process, the physical structure of martensite changes, and the corrosion resistance and toughness of the weld metal are improved compared with the base material. A combination of tempered martensite and bainite in the HAZ and residual austenite during weld solidification is shown in Figure 5d. Tempered martensite provides high strength, while bainite and retained austenite enhance toughness and ductility. This combination optimizes the mechanical

properties of the HAZ by achieving a balance between hardness, strength, and impact resistance. Obvious differences in the microstructure of these regions can significantly affect the mechanical properties of the welded joint, affecting factors such as strength, toughness, and fracture resistance. Enable welded joints to overcome the challenges posed by the harsh underwater environment.

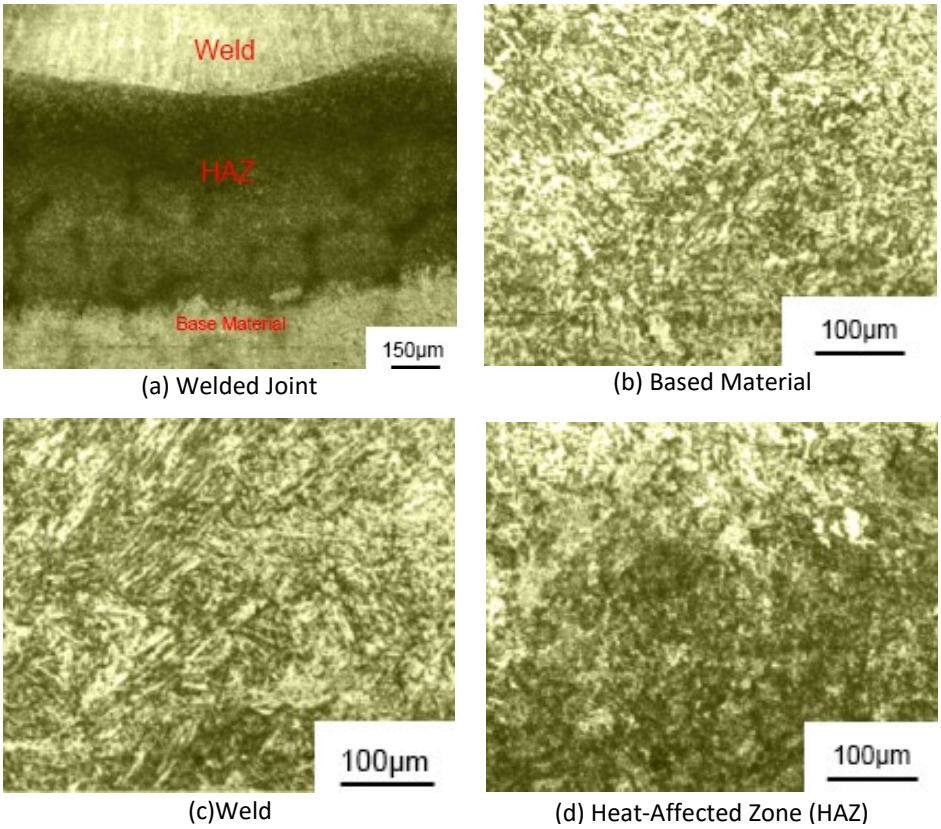

(a) Welded Joint (b) Based Material

(c)Weld (d) Heat-Affected Zone (HAZ)

Fig. 5. Microstructure of a welded joint

3.3 Microhardness of Welded Joints

Micro Vickers hardness tester (Model HV-30) was used for microhardness measurement. Test samples were loaded on 9.8 N for 10 s. In each interval of 0.1 mm apart, the measurement of hardness was taken and the data was analyzed to identify the microhardness of the different positions, as shown in Figure 6. The microhardness of the weld region has the peak values, which is due to the formation of martensite in the microstructure during rapid cooling of the weld metal. The microhardness of the HAZ is lower than the one of the weld areas. The microstructure of the HAZ is austenite, however, the microhardness of the HAZ is significantly affected by the distance from the center of the weld, where the hardness is higher at the HAZ zone which is closer to the weld area. Among the three regions in the test, the base material has the lowest microhardness as it contains a large amount of ferrite in the microstructure. However, the joint organization of base material has no softening phenomenon as the UGNW method is characterized by welding heat input that is small on the welded joints without a softening phenomenon.

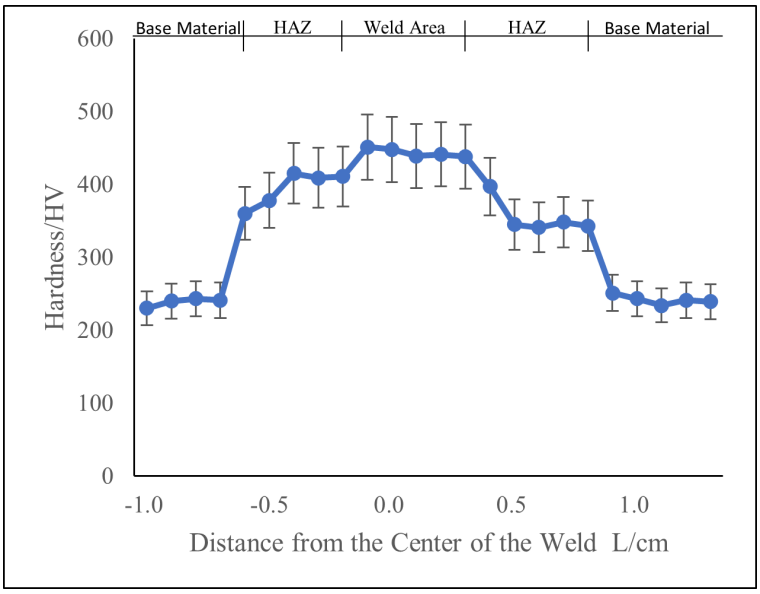

Fig. 6. Microhardness diagram

3.4 Air Bubbles Analysis

Air bubbles are a common phenomenon in the welding process. The presence of air bubbles can focus the stress concentration and therefore cause the weld quality to be significantly reduced. As a result of the metallurgical reaction in the welding process, the formation of porosity can be caused by the water content of flux bands or the air is too large. The high temperature of welding will turn the water inside the flux bands into gas. If the welding speed is too fast while the heat input to the weld is not sufficient, the molten pool will cool down before the gas can properly escape from the weld, then air bubbles were formed. Moreover, if the carbonate content in the flux band is insufficient, then less carbon dioxide will be produced by the melting process and therefore it cannot achieve the role of welding protection. Thus, the air can flow into the molten pool and cause formation of air bubbles after the weld metal cooling down. The air bubbles in the welding defects are shown in Figure 7(a).

To reduce or avoid the formation of air bubbles, the welding production process is a crucial factor. Therefore, the operator needs to understand the source of air bubbles formation. The sources include the moisture in the deoxygenation reaction, which produces the hydrogen holes, and as well as the air trapped into the molten pool during the metallurgical reaction. In this study, changing the composition of the flux band and increasing the proportion of marble and fluorite cannot solve the air bubbles in the weld and on the weld surface, but when a certain proportion of quartz sand is added to the composition of the flux band, the surface of the weld shows a clear metallic cluster, and the air bubbles are reduced significantly. After modification of the flux band, the weld metal as shown in Figure 7(b) was obtained, where the porous hole in the weld is not obviously observed**.**

Table 3 shows the effect of welding current and voltage on weld metal. When both current and voltage are too low, the weld metal may not adequately penetrate into the base material, resulting in a weak joint that is susceptible to failure under stress. The weld bead may become narrow and convex, lacking proper fusion with the base material. This results in poor mechanical strength. The molten metal may not adequately fuse with the base material or the previous weld bead, creating weak spots and possibly incomplete fusion defects. Low heat input can cause the weld pool to solidify too quickly, trapping gases and causing air bubbles within the weld, compromising its integrity. The weld bead may appear uneven and irregular due to unstable arc conditions, resulting in inconsistent

weld quality. Low current and voltage can cause arc instability, increasing spatter and causing an uneven weld surface.

When both current and voltage are too high, an over-melting effect can occur. The weld metal may penetrate too deeply into the base material, resulting in burn-through. The weld bead may become too wide and flat, reducing reinforcement strength and resulting in a weak joint. High current and voltage can increase spatter, producing small droplets of molten metal scattered around the weld area, which may require additional cleanup. High heat input can cause air bubbles and hot cracks in the weld because gases are trapped during the solidification process.

After experimental verification, the best welding results are obtained with a welding current of 200-230A and a welding voltage of 21.5-23V. Appropriate welding parameters ensure sufficient penetration, so the weld metal is well integrated with the base material to form a strong joint. A balanced weld with good enhancement and a smooth transition to the base material is achieved. Minimal spatter reduces cleanup time and improves overall weld quality. Maintaining a controlled HAZ maintains material properties and minimizes deformation and residual stress.

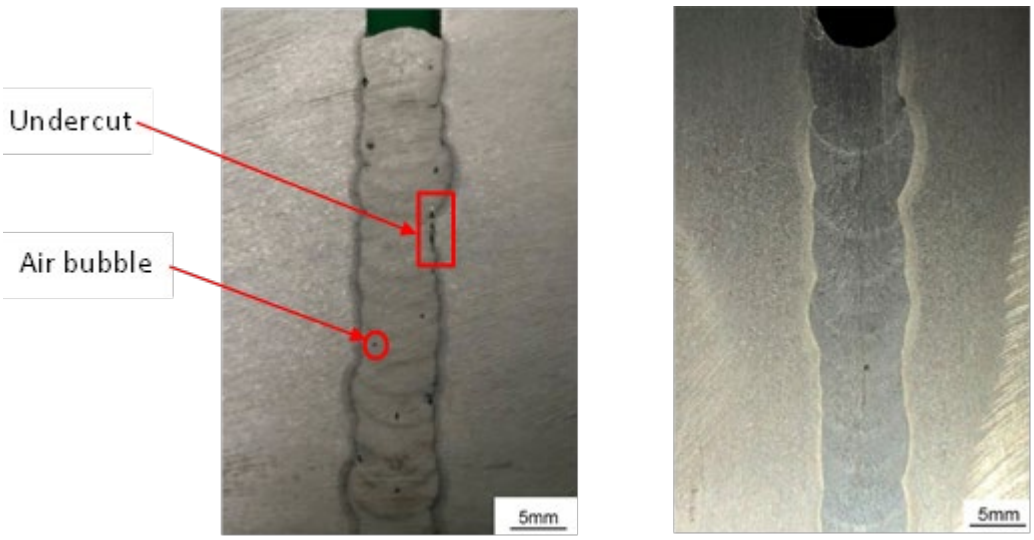

Fig. 7. (a) Air bubbles in the weld defects, (b) Formation of an air bubble in the weld metal is not obvious after modification of flux band

Table 3
Effect of welding current and voltage on weld metal

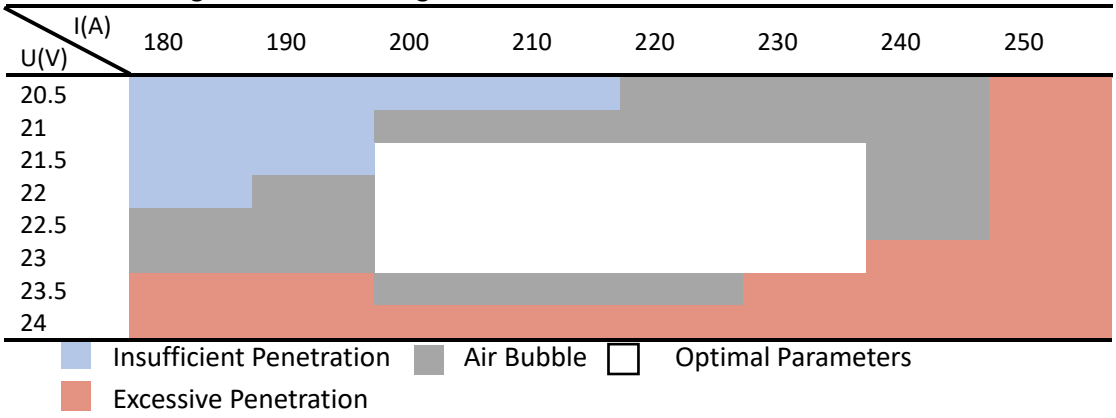

4. Conclusion

In this study, the feasibility of the ultra-narrow gap welding method for cast steel pipes is determined by analyzing the role of flux bands in the welding process and by observing the formability and organization of the weld seam at the macro and micro levels. By analyzing the changes in various welding parameters obtained from the experimental results, the influence rules on UNGW are obtained. The main findings of the experimental results are:

i. The optimal range for the welding parameters is a welding voltage of 22V, welding current of 200-230A, and welding speed of 8.25-9mm/s.
ii. Microstructure analysis showed a mixture of tempered martensite, bainite, and retained austenite at Heat Affected Zones.
iii. Microhardness results demonstrated no softening at the welded joints.
iv. Composition of the flux band can be manipulated to improve the fusion of air bubbles and side walls.

Compared with traditional welding, UNGW has the unique advantages of high efficiency, low cost, and excellent joint mechanical properties, which reflects the importance of UNGW for the application in underwater pipelines. In the future works, UNGW can be further optimized for potential applications in other engineering applications.

References

[1] Zhixin, W. E. N., W. A. N. G. Jianjun, W. A. N. G. Zhaoming, H. E. Zhengjun, S. O. N. G. Chengpeng, L. I. U. Xiaobing, Ningning Zhang, and J. I. Tianyu. "Analysis of the world deepwater oil and gas exploration situation." *Petroleum Exploration and Development* 50, no. 5 (2023): 1060-1076. https://doi.org/10.1016/S1876-3804(23)60449-5

[2] Zhang, Yu, Peng Xu, Mingbiao Xu, Lei Pu, and Xinying Wang. "Properties of Bentonite Slurry Drilling Fluid in Shallow Formations of Deepwater Wells and the Optimization of Its Wellbore Strengthening Ability While Drilling." *ACS omega* 7, no. 44 (2022): 39860-39874. https://doi.org/10.1021/acsomega.2c03986

[3] Alsebai, Fouzi, Hooi-Siang Kang, Omar Yaakob, and Muhammad Noor Afiq Witri Muhammad Yazid. "Review of resources from the perspective of wave, tidal, and ocean thermal energy conversion." *Journal of Advanced Research in Applied Sciences and Engineering Technology* 30, no. 3 (2023): 127-149. https://doi.org/10.37934/araset.30.3.127149

[4] Adnan, Nur Fatimah, Kee Quen Lee, Hooi Siang Kang, Keng Yinn Wong, and Hui Yi Tan. "Preliminary investigation on the energy harvesting of vortex-induced vibration with the use of magnet." *Progress in Energy and Environment* (2022): 1-7. https://doi.org/10.37934/progee.21.1.17

[5] Feng, Qing-Shan, and Yan-Hui Zhang. "Review and discussion of strength mismatch of girth welds in high strength pipelines." *International Journal of Pressure Vessels and Piping* (2023): 105118. https://doi.org/10.1016/j.ijpvp.2023.105118

[6] Xu, Pu, Zhixin Du, Fuyun Huang, and Ahad Javanmardi. "Numerical simulation of deepwater S-lay and J-lay pipeline using vector form intrinsic finite element method." *Ocean Engineering* 234 (2021): 109039. https://doi-org.ezproxy.utm.my/10.1016/j.oceaneng.2021.109039

[7] Kah, Paul, Madan Shrestha, and Jukka Martikainen. "Trends in joining dissimilar metals by welding." *Applied Mechanics and Materials* 440 (2014): 269-276. https://doi.org/10.4028/www.scientific.net/AMM.440.269

[8] Barnabas, S. Godwin, S. Rajakarunakaran, G. Satish Pandian, A. Muhamed Ismail Buhari, and V. Muralidharan. "Review on enhancement techniques necessary for the improvement of underwater welding." *Materials Today: Proceedings* 45 (2021): 1191-1195. https://doi-org.ezproxy.utm.my/10.1016/j.matpr.2020.03.725

[9] Valiulin, I. R., E. A. Solovmev, A. S. Fik, O. Yu Elagina, and N. N. Nikolaeva. "Effect of welding technology on the mechanical properties of welded joints in pipes for deep water offshore gas pipelines." *Welding International* 31, no. 5 (2017): 363-368. https://doi.org/10.1080/09507116.2016.1263457

[10] Kotari, Sairam, Eshwaraiah Punna, SM Gangadhar Reddy, and S. Venukumar. "Experimental Investigation and Micro Structural Characteristics of GTAW and FSW Welded Dissimilar Aluminum Alloys." In *IOP Conference Series: Materials Science and Engineering*, vol. 998, no. 1, p. 012036. IOP Publishing, 2020. https://www.sci-hub.ee/10.1088/1757-899X/998/1/012036

[11] Kumar, G. Sathish, S. Saravanan, A. V. Balan, J. Oscar, R. Ragunath, and M. Ramesh. "Influence of FCAW process parameters in super duplex stainless steel claddings." *Materials Today: Proceedings* 21 (2020): 63-65. https://doi.org/10.1016/j.matpr.2019.05.362
[12] Jiang, Xu, Daqian Cao, Xuhong Qiang, and Chunli Xu. "Study on fatigue performance of steel bridge welded joints considering initial defects." *Journal of Constructional Steel Research* 212 (2024): 108309. https://doi.org/10.1016/j.jcsr.2023.108309
[13] Reeves, K. D., and T. Tran. "Practical Considerations for Standard Flaw Acceptance Criteria on Subsea Pipeline Girth Welds." In *Offshore Technology Conference Asia*, p. D031S040R003. OTC, 2016. https://doi.org/10.4043/26466-MS
[14] Li, Mingfei, Song Lin, and Jian Chen. "Study on quantitative risk assessment of girth weld failure of natural gas pipeline based on reliability." (2022): 228-235. https://doi.org/10.1049/icp.2022.2874
[15] Zhu, Yao, Zhiquan Xing, Wanpeng Zhang, Chuanxiang Xiong, Yu Chen, Wei Chen, and Lizhong Jiang. "Behavior of longitudinal-seam steel tubular columns with crack defect in weld." *Journal of Constructional Steel Research* 212 (2024): 108286. https://doi.org/10.1016/j.jcsr.2023.108286
[16] Xing, Jiduo, Tarek Zayed, and Shihui Ma. "Corrosion-based failure analysis of steel saltwater pipes: A Hong Kong case study." *Engineering Failure Analysis* 161 (2024): 108266. https://doi.org/10.1016/j.engfailanal.2024.108266
[17] Yusof, F., and M. F. Jamaluddin. "Welding defects and implications on welded assemblies." (2014): 125-134. https://doi.org/10.1016/B978-0-08-096532-1.00605-1
[18] Oliveira, J. P., T. G. Santos, and R. M. Miranda. "Revisiting fundamental welding concepts to improve additive manufacturing: From theory to practice." *Progress in Materials Science* 107 (2020): 100590. https://doi.org/10.1016/j.pmatsci.2019.100590
[19] Liu, Chuan, Jiawei Yang, Yifeng Shi, Qiang Fu, and Yong Zhao. "Modelling of residual stresses in a narrow-gap welding of ultra-thick curved steel mockup." *Journal of Materials Processing Technology* 256 (2018): 239-246. https://doi.org/10.1016/j.jmatprotec.2018.02.024
[20] Yang, Tao, Junfeng Liu, Yuan Zhuang, Kai Sun, and Weilin Chen. "Studies on the formation mechanism of incomplete fusion defects in ultra-narrow gap laser wire filling welding." *Optics & Laser Technology* 129 (2020): 106275. https://doi.org/10.1016/j.optlastec.2020.106275
[21] Lei, Zhen, Hao Cao, Xiufang Cui, Yiming Ma, Lin Li, and Qing Zhang. "A novel high efficiency narrow-gap laser welding technology of 120 mm high-strength steel." *Optics and Lasers in Engineering* 178 (2024): 108232. https://doi.org/10.1016/j.optlaseng.2024.108232
[22] Mohanty, Uttam Kumar, Angshuman Kapil, Yohei Abe, Tetsuo Suga, Manabu Tanaka, and Abhay Sharma. "A resource-efficient process design for heavy fabrication: A case of single-pass-per-layer narrow gap welding." *Sustainable Materials and Technologies* 33 (2022): e00488. https://doi.org/10.1016/j.susmat.2022.e00488
[23] Li, Ruoyang, Jun Yue, Ran Sun, Gaoyang Mi, Chunming Wang, and Xinyu Shao. "A study of droplet transfer behavior in ultra-narrow gap laser arc hybrid welding." *The International Journal of Advanced Manufacturing Technology* 87 (2016): 2997-3008.https://doi.org/10.1007/s00170-016-8699-9
[24] Gong, Lian. "Interaction mechanism of flux band and arc in ultra-narrow gap welding." (2017). https://www.sci-hub.ee/10.12073/j.hjxb.20160412002
[25] Chen, Hao, Ning Guo, Xianghua Shi, Yongpeng Du, Jicai Feng, and Guodong Wang. "Effect of water flow on the arc stability and metal transfer in underwater flux-cored wet welding." *Journal of Manufacturing Processes* 31 (2018): 103-115. https://doi-org.ezproxy.utm.my/10.1016/j.jmapro.2017.11.010
[26] Gong, Lian, Liang Zhu, and Hong Xiang Zhou. "Effect on hardness and microstructures of rail joint with ultra-narrow gap arc welding by post weld heat treatment." *Key Engineering Materials* 737 (2017): 90-94. https://doi.org/10.4028/www.scientific.net/KEM.737.90
[27] Yin, Tie, Jinpeng Wang, Hong Zhao, Lun Zhou, Zenghuan Xue, and Hehe Wang. "Research on filling strategy of pipeline multi-layer welding for compound narrow gap groove." *Materials* 15, no. 17 (2022): 5967. https://doi.org/10.3390/ma15175967
[28] Wang, Lei, Yongtao Liu, Yuechao Li, Mengkun Zhu, and Jisen Qiao. "Study on mechanism of the effect of Al element on the arc shape and molten pool fluctuation pattern in flux bands constricting arc welding (FBCA)." *Journal of Manufacturing Processes* 101 (2023): 882-891. https://doi-org.ezproxy.utm.my/10.1016/j.jmapro.2023.06.044
[29] Dak, Gaurav, Navneet Khanna, and Chandan Pandey. "Study on narrow gap welding of martensitic grade P92 and austenitic grade AISI 304L SS steel for ultra-supercritical power plant application." *Archives of Civil and Mechanical Engineering* 23, no. 1 (2022): 14. https://doi.org/10.1007/s43452-022-00540-3
[30] TANG, Guoxi, Liang ZHU, Aihua ZHANG, Hui ZHOU, Ning GUO, and Yi ZHOU. "Analysis of interaction mechanism between feeding flux sheet and arc in ultra-narrow gap welding." *Transactions of The China Welding Institution* 44, no. 3 (2023): 54-60. https://doi.org/10.12073/j.hjxb.20220429002

[31] He, Weilong, Ping Wang, Aihua Zhang, Jing Ma, Shengming Ma, and Yanpeng Feng. "Detection of arc shape in ultra-narrow gap welding based on improved YOLOv5s." In *2022 4th International Conference on Industrial Artificial Intelligence (IAI)*, pp. 1-6. IEEE, 2022. https://doi.org/10.1109/IAI55780.2022.9976556

[32] Wang, Lei, Jisen Qiao, Zhenwen Chen, Liang Zhu, and Jianhong Chen. "Method exploration of flux bands constricting arc welding for high-strength steel T-joints." *The International Journal of Advanced Manufacturing Technology* 105 (2019): 2447-2460. https://doi.org/10.1007/s00170-019-04471-x